


Cite this: *RSC Adv.*, 2024, 14, 25889

Ti and Zr complexes bearing guanidine-phenolate ligands: coordination chemistry and polymerization studies†

V́ctor Flores-Romero,  Jesse LeBlanc,  Zichuan Chen and Gino G. Lavoie *

A series of group 4 bis(isopropoxide) complexes $M[N^{\wedge}O]_2(O^iPr)_2$, stabilized by guanidine-phenolate $N^{\wedge}O$ ligands, have been prepared and used as catalysts for the polymerization of unpurified *rac*-lactide under solvent-free conditions at 130 °C. The resulting polylactic acid (PLA) presented heterotactic bias ($P_r = 0.56\text{--}0.62$) with molecular weights similar to those obtained in control experiments with $Zr(O^iPr)_4 \cdot iPrOH$, $Ti(O^iPr)_4$, and $Sn(Oct)_2$. The molecular weights were lower than expected for living polymerization due to chain transfer and/or transesterification. Zr complexes were more active than the Ti homologues, with rate constants ranging from $1.17\text{--}3.21 \times 10^{-4} \text{ s}^{-1}$, comparable to that observed with the free guanidine-phenol ligands. The corresponding bis(guanidine-phenolate) titanium dichloride complexes $Ti[N^{\wedge}O]_2Cl_2$ were also prepared and tested in ethylene polymerization. The low activity (up to $1.1 \text{ kg}_{PE} \text{ mol}^{-1} \text{ h}^{-1}$) was associated to the strong electron-donating ability of the guanidine moiety and to the *trans*-*N,N*-*cis*-*O,O*-*cis*-*Cl,Cl* coordination mode of the guanidine-phenolate ligand.

Received 16th July 2024
Accepted 5th August 2024

DOI: 10.1039/d4ra05146g

rsc.li/rsc-advances

Introduction

In recent years, polylactic acid (PLA) has attracted much interest as a biodegradable polymer that uses renewable resources, such as corn starch and sugar beet, as feedstock.^{1–3} Select microstructures of PLA have shown mechanical properties similar to fossil fuel-based polymers, and have found applications in consumer materials such as packaging, plastic bottles, and fibers.^{3–7} PLA has also been used in drug delivery systems and orthopaedic fixation devices.^{8,9}

Although PLA can be synthesized by polycondensation of lactic acid, this process is not industrially viable due to the ultrapure conditions and high conversion needed to achieve high molecular weight polymers. Thus, the industry relies on the metal-mediated ring-opening polymerization (ROP) of lactide, which exhibits more favorable kinetics for the production of high molecular weight polymers.^{10–13} Polylactic acid is commercially produced at elevated temperatures, in the melt phase, in the absence of solvent, with tin octanoate ($Sn(Oct)_2$) as the most commonly used catalyst.^{14–17} Tin octanoate however does not impart stereoregularity to the polymer mainchain, resulting in a material with poor bulk properties, thus limiting the scope of applications of the material. Under the

polymerization conditions used by the industry, $Sn(Oct)_2$ however also catalyzes transesterification, leading to poor control of molecular weights and molecular weight distribution. Furthermore, traces of toxic tin in the polymer limit possible applications in medical devices.^{3,18}

Catalytic systems containing nitrogen-donor ligands and less toxic metals such as alkali and alkaline earth metals,^{19–21} iron,^{22,23} and zinc^{24–30} have proven to be effective for the ROP of cyclic esters. In particular, group 4 metals have shown excellent activities among these non-toxic metals,^{31–33} polymerizing lactide by a coordination-insertion mechanism.^{34–37} Zirconium acetylacetonate has also proven effective in the production of PLA and copolymers by ring-opening polymerization of lactides and other cyclic esters.³⁸ Related zirconium diketiminate complexes were found to be very active, with the substituents on the two nitrogen atoms used to modulate the sterics and electronics of the catalysts.³⁹ Other nitrogen-donor ligands, such as phenoxy-imine, phenoxy-amine, pyrrole, and pyridine, have also drawn much interest.^{24,40–46} Davidson developed group 4 metal alkoxides supported by a tetradentate phenoxy-amine ligand to polymerize *rac*-lactide under solvent-free conditions, yielding atactic PLA.⁴⁷ In contrast, zirconium catalysts of chiral phenoxy-imine ligands produced moderately heterotactic PLA under both solvent-free conditions (130 °C) and in toluene (80 °C).⁴⁸

Neutral N-heterocyclic imines and the corresponding anionic iminates, especially those formally based on the corresponding N-heterocyclic carbenes (NHC), have recently drawn much attention as N-based spectator ligands due to the ability to tailor their steric and electronic contributions. These cyclic

York University, 4700 Keele Street, Toronto, Ontario, M3J 1P3, Canada. E-mail: glavoie@yorku.ca

† Electronic supplementary information (ESI) available: ¹H and ¹³C NMR spectra, plots to calculate k_{app} , and crystal and structure refinement data (PDF). CCDC 2345354–2345357. For ESI and crystallographic data in CIF or other electronic format see DOI: <https://doi.org/10.1039/d4ra05146g>



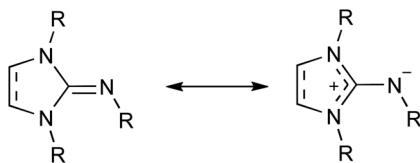


Fig. 1 Mesomeric forms of cyclic guanidines.

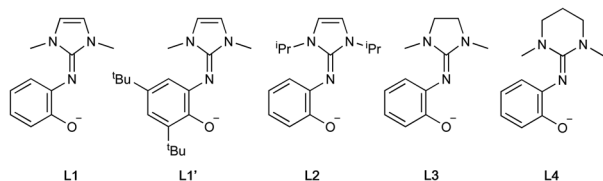


Fig. 2 Structure of guanidine-phenolate ligands herein explored.

guanidines exist as two mesomeric forms, illustrating electron delocalization from the endocyclic nitrogen atoms to the exocyclic atom (Fig. 1). The electron density on this exocyclic nitrogen, and thus its electron-donating ability to metal, can be modulated by modifying the NHC scaffold itself, with its steric contributions to the system altered through the substituents on the endocyclic nitrogen atoms.

A decade ago, our group reported the first chelating anionic guanidine-ethenolate ligands and their coordination to group 4 metals.⁴⁹ The corresponding titanium complex showed good activity in ethylene polymerization. Since then, other guanidine-based bidentate ligands, both neutral and anionic, have been reported with the metal complexes used as catalysts in both olefin and lactide polymerizations.^{50–53} We were especially intrigued by the guanidine-phenolate ligand systems reported by Eisen and exclusively coordinated to group 10 nickel and palladium for homo- and copolymerization of norbornene. These ligands in fact closely resemble the phenoxy-imine ligands used in group 4 metal complexes used in both olefin and lactide polymerization.^{54–56}

On this basis, chelating ligands containing a neutral cyclic guanidine donor paired with an anionic phenolate appeared to

be excellent candidates for complexation to group 4 metals and for study in both lactide and olefin polymerizations. Hence, we herein describe the synthesis and characterization of titanium and zirconium alkoxide and chloride complexes of such ligands with imidazole-, imidazolidine- and tetrahydropyrimidine-based guanidines (Fig. 2). These guanidines offer the opportunity to deconvolute the steric and electronic effects and study the catalytic performance of the corresponding metal complexes.

Results and discussion

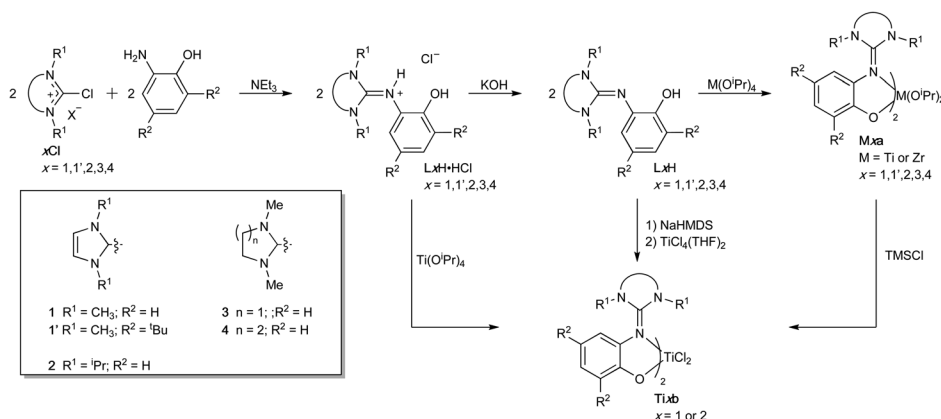
Synthesis of proligands

The guanidine-phenol hydrochloride salts **LxH**·HCl (wherein **x** = 1, 1', 2, 3 and 4) were prepared by reacting the chloro halide salt **xCl** with 2-aminophenol or the corresponding *tert*-butyl derivative (Scheme 1).⁵² Deprotonation of these salts with KOH gave the corresponding guanidine-phenol **LxH** in 63–90% yield. Despite the formal C=N_{exo} double bond of the guanidine, NMR spectra of both the phenol and the hydrochloride salt showed magnetically-equivalent R¹ groups, consistent with free rotation about the C=N_{exo} due to electron delocalization from the N_{endo} lone pairs. This contrasts with restricted rotation observed in our related systems with diacylated imidazolidines, wherein the acyl groups compete for the π-electron density.⁵⁰

Synthesis of bis(guanidine-phenolate) Ti and Zr complexes

The titanium and zirconium bis(isopropoxide) complexes **Mxa** were respectively prepared in excellent yields (>85%) at 60 °C by addition of guanidine-phenol **LxH** to Ti(O^{*i*}Pr)₄ or Zr(O^{*i*}Pr)₄·^{*i*}PrOH in a 2 : 1 stoichiometric ratio (Scheme 1). The ¹H NMR spectra of all complexes are consistent with the structure proposed and showed the generation of one single isomer. Most titanium complexes showed broad resonances for the aliphatic protons, due to a sterically crowded coordination sphere.

The solid-state molecular structures of complexes **Ti3a**, **Zr3a**, and **Ti4a** are shown in Fig. 3. All complexes are six-coordinate with the isopropoxide groups in a *cis* arrangement. Selected bond distances and angles are given in Table 1. The guanidine-phenolate binds to the metal in a bidentate fashion to give the



Scheme 1 Synthesis of ligand and group 4 complexes.

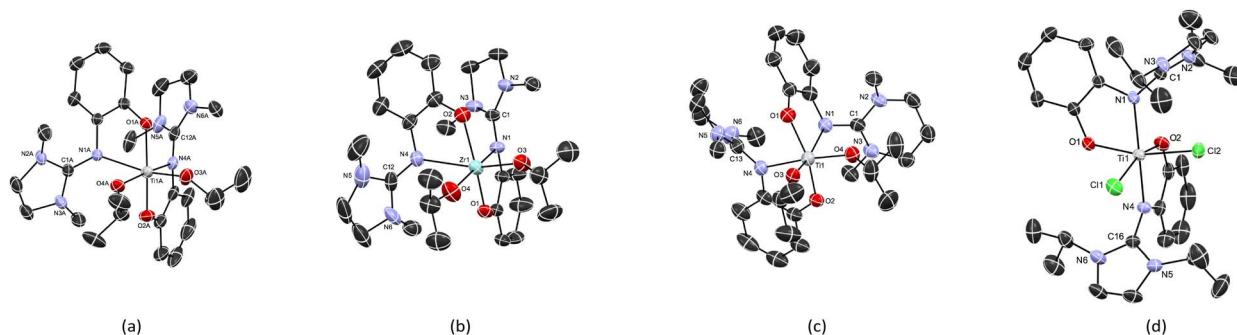


Fig. 3 Solid-state structures of (a) **Ti3a**, (b) **Zr3a**, (c) **Ti4a** and (d) **Ti2b**. Hydrogen atoms and solvent have been omitted for clarity. ORTEP drawn at 50% probability.

Table 1 Selected bond distances [Å] and angles [°] for complexes **Ti3a**, **Zr3a**, **Ti4a** and **Ti2b**

	Ti3a	Zr3a	Ti4a		Ti2b
M–O1	1.9182(12)	2.061(3)	1.939(3)	Ti–O1	1.9098(14)
M–O2	1.9245(14)	2.061(3)	1.937(3)	Ti–O2	1.9277(14)
M–O3	1.8103(14)	1.944(3)	1.809(3)	Ti–Cl1	2.3783(6)
M–O4	1.8466(13)	1.971(3)	1.850(3)	Ti–Cl2	2.3883(6)
M–N1	2.3724(14)	2.386(3)	2.281(4)	Ti–N1	2.0664(15)
M–N4	2.2738(14)	2.456(3)	2.275(4)	Ti–N4	2.0666(14)
C1–N1	1.323(2)	1.328(4)	1.343(6)	C1–N1	1.372(2)
C1–N2	1.368(2)	1.342(5)	1.354(6)	C1–N2	1.342(2)
C1–N3	1.350(2)	1.362(5)	1.348(6)	C1–N3	1.345(2)
C12–N4	1.322(2)	1.329(5)	1.335(6)	C16–N4	1.369(2)
C12–N5	1.374(2)	1.348(6)	1.350(6)	C16–N5	1.343(2)
C12–N6	1.339(3)	1.365(6)	1.350(6)	C16–N6	1.345(2)
O1–M–O2	158.35(6)	151.00(10)	158.03(15)	Cl1–M–Cl2	87.84(2)
O3–M–O4	98.28(6)	96.69(12)	96.19(15)	O1–M–O2	94.38(6)
N1–M–N4	84.91(5)	85.29(10)	86.81(14)	N1–M–N4	167.97(6)
N1–M–O1	74.68(5)	72.08(10)	75.94(14)	N1–M–Cl1	104.59(5)
N4–M–O2	75.24(6)	71.49(11)	75.02(14)	N1–M–Cl2	85.10(6)
ρ^a	0.97	0.98	0.99	ρ^a	1.00

^a Averaged value of both guanidine fragments and calculated as reported in the literature.⁵⁰

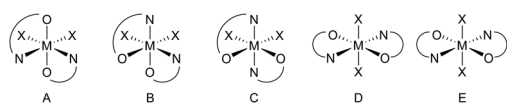


Fig. 4 Possible isomers (excluding enantiomers) for bis(guanidine-phenolate) six-coordinate complexes.

cis-N,N-trans-O,O diastereomer with average bite angles of 74.96° and 75.48° for **Ti3a** and **Ti4a**, respectively. As expected, a smaller bite angle of 71.79° was observed in the corresponding zirconium complex **Zr3a**. The O1–M–O2 bond angles deviates from linearity, at 158.35(6)°, 158.03(15) and 151.00(10)° for **Ti3a**, **Ti4a** and **Zr3a**, respectively. The M–OⁱPr bond lengths range from 1.809(3) to 1.971(3) Å, consistent with analogous group 4 complexes of phenoxy-imine ligands with the same stereo-arrangement.⁵⁷ The structural parameter ρ values of 0.97–0.99 indicate extended electron delocalization within the guanidine moiety.

DFT calculations on all five possible isomers of the X-ray characterized bis(isopropoxide) complexes **Ti3a**, **Zr3a** and **Ti4a** were performed (Fig. 4), using B3LYP-D3(BJ)/def2-SVP for geometry optimization and B3LYP-D3(BJ)/def2-TZVPP for single-point energy calculations.⁴⁴ Isomer **A** was predicted to be the most stable isomer, consistent with the solid state structures, by 1–28 kJ mol^{−1} compared to the *cis* isopropoxide isomers **B** and **C** (Table 2), and by 35–70 kJ mol^{−1} for the much less stable *trans* isopropoxide isomers **D** and **E** (Table S1†). Considering the large unfavorable energies for the *trans* isopropoxide isomers **D** and **E**, computations on complexes not characterized by X-ray diffraction were then performed on only diastereomers **A–C**. The calculations predict the isomer **A** (*cis-N,N-trans-O,O*) to be the most stable isomer.

Replacing the methyl groups on the endocyclic nitrogen in **Ti1a** with larger isopropyl substituents in **Ti2a** resulted in an energy difference between isomers **A** and **C** to be only 1 kJ mol^{−1}. In most cases, isomer **B** (*cis-N,N-cis-O,O*) is predicted to be the least stable diastereomer, with the exception of **Ti1a**, **Ti3a** and **Zr3a**, which are 5–14 kJ mol^{−1} more stable than isomer **C**. Similar results have been observed for the analogous bis(phenoxy-imine) group 4 systems adopting preferentially the *N,N-cis-O,O-trans* ligand arrangements (isomer **A**) unless bulky substituents are present.^{57,58}

The titanium dichloride complexes **Ti1b**, **Ti1'b**, and **Ti2b** were prepared by reaction of 2 equivalents of the guanidinium

Table 2 Energies (kJ mol^{−1}) of isomer **B** and isomer **C** of the bis(guanidine-phenolate) group 4 alkoxide complexes, relative to that of the more stable isomer **A**

Complex	Isomer B (<i>cis-N,N-cis-O,O</i>)	Isomer C (<i>trans-N,N-cis-O,O</i>)
Ti1a	35	45
Zr1a	36	28
Ti1'a	43	39
Zr1'a	38	25
Ti2a	34	1
Zr2a	41	17
Ti3a	5	15
Zr3a	1	15
Ti4a	28	27
Zr4a	33	25



Table 3 Energies (kJ mol⁻¹) of isomers **A** and **B** for bis(guanidine-phenolate) titanium dichloride complexes, relative to that of the more stable isomer **C**

Complex	Isomer A <i>cis-N,N-trans-O,O</i>	Isomer B <i>cis-N,N-cis-O,O</i>
Ti1b	1	36
Ti1'b	6	21
Ti2b	18	55

chloride salt **LxH**·HCl with Ti(OⁱPr)₄ in excellent yields (>90%) (Scheme 1). ¹H NMR spectra of these complexes showcase one single set of resonances, consistent with the presence of only one isomer, with magnetically-inequivalent protons for the alkyl substituents on the endocyclic nitrogen atoms. Alternatively, these dichloride complexes could also be prepared from reaction of either the corresponding bis(isopropoxide) complexes with TMSCl or TiCl₄(THF)₂ with the sodium guanidine-phenolate salt, giving products that were undistinguishable spectroscopically.

The X-ray structure of **Ti2b** exhibits a distorted octahedral geometry, with a *trans-N,N-cis-O,O* ligand arrangement (isomer **C**; Fig. 3 and 4, Table 1). This contrasts with the *cis-N,N-trans-O,O* ligand arrangement (isomer **A**) observed for the bis(isopropoxide) complexes **Ti3a**, **Ti4a** and **Zr3a** and normally observed for bis(phenoxy-imine) titanium complexes. In the latter case, the *trans-N,N-cis-O,O* arrangement (isomer **C**) is limited to ligands with sterically-demanding substituents on the nitrogen.^{54,58} Interestingly, our earlier DFT calculations (*vide supra*) on the bis(isopropoxide) complexes predicted this arrangement to be the second most stable isomer. However, DFT calculations of isomers **A**, **B** and **C** for the dichloride complexes **Ti1b**, **Ti1'b**, and **Ti2b** predicted isomer **C** to be more stable than isomers **A** and **B** by 1–18 kJ mol⁻¹ and 21–

55 kJ mol⁻¹, respectively (Table 3). These calculations are in agreement with the solid state structure of **Ti2b** and further illustrate the important effect of bulky substituents on the preferred arrangement of the guanidine-phenolate (and phenoxy-imine) ligands.

Ring-opening polymerization of *rac*-lactide with metal alkoxide complexes

All complexes were tested in the ring-opening polymerization of *rac*-lactide. Polymerizations were performed in the absence of any solvent at 130 °C with a 100 : 1 stoichiometric ratio of lactide to catalyst, using unpurified monomer (Table 4). All complexes gave full conversion within 6 h. The polymerization rate constants were obtained by monitoring the consumption of the monomer over time using ¹H NMR spectroscopy. On average, zirconium complexes are 28% more active than the corresponding titanium homologues, with *k*_{app} average values of 1.17–1.82 × 10⁻⁴ s⁻¹ and 1.39–3.21 × 10⁻⁴ s⁻¹ for Ti and Zr complexes, respectively. This is consistent with other group 4 catalytic systems and attributed to an easier coordination of the monomer to the larger zirconium metal and a more nucleophilic alkoxide ligand.⁴³ While these rate constants compare favorably to those determined with Ti(OⁱPr)₄ (0.53 × 10⁻⁴ s⁻¹) and Zr(OⁱPr)₄·ⁱPrOH (0.28 × 10⁻⁴ s⁻¹), the activity is approximately an order of magnitude less active than that observed for Sn(Oct)₂ (12.4 × 10⁻⁴ s⁻¹).

The number-average molecular weight (*M*_n) of the polymers was determined by ¹H NMR end-group analysis and gel permeation chromatography (GPC) with values of 700–2200 Da and 700–3300 Da, respectively. The weight-average molecular weight (*M*_w) was determined by diffusion-ordered spectroscopy (DOSY) and GPC with values of, 1200–3300 Da, and 900–4700 Da, respectively (Table 4).^{59–61} These values are comparable to those observed with the control experiments using Ti(OⁱPr)₄,

Table 4 Solvent-free polymerization of *rac*-lactide^a

Entry	Catalyst	<i>k</i> _{app} ^b (10 ⁻⁴ s ⁻¹)	<i>M</i> _n ^c (Da)	<i>M</i> _w ^e (Da)	<i>D</i> ^f	<i>M</i> _n ^d (Da)	<i>M</i> _w ^d (Da)	<i>D</i> ^g	<i>P</i> _r
1	Ti1a	1.22	700	1600	2.3	1400	1900	1.4	0.63
2	Ti1'a	1.82	1400	2400	1.7	2700	4000	1.5	0.62
3	Ti2a	1.56	1400	1900	1.4	2200	2900	1.3	0.56
4	Ti3a	1.44	700	1500	2.1	1300	1600	1.2	0.62
5	Ti4a	1.17	1000	1900	1.9	1600	2100	1.3	0.56
6	Zr1a	1.78	1800	3000	1.6	2700	3500	1.3	0.56
7	Zr1'a	2.24	1100	2100	1.9	1700	2400	1.4	0.58
8	Zr2a	2.11	1200	1900	1.6	1600	2100	1.3	0.58
9	Zr2a^h	2.54	1100	2400	2.2	1700	2300	1.4	0.58
10	Zr2aⁱ	3.21	1200	1900	1.6	1500	2100	1.4	0.58
11	Zr3a	1.63	900	1700	1.8	1500	1900	1.3	0.62
12	Zr4a	1.39	1500	2600	1.7	2300	2900	1.3	0.58
13	L2H^j	2.49	1400	3000	2.1	1700	2500	1.5	0.48
14	Sn(Oct) ₂	12.4	2200	3300	1.5	3300	4700	1.4	0.68
15	Ti(O ⁱ Pr) ₄	0.53	700	1500	2.1	700	900	1.3	0.50
16	Zr(O ⁱ Pr) ₄ · ⁱ PrOH	0.28	700	1600	2.1	1000	1200	1.2	0.50

^a All polymerization were carried out at 130 °C within 6 h and a lactide-to-catalyst stoichiometric ratio of 100 : 1. ^b An average standard error of 5% was calculated for the rate constants. ^c Determined by ¹H NMR end-group analysis assuming –OⁱPr as chain-end. ^d Determined by GPC in THF. ^e Determined by DOSY NMR in C₆D₆. ^f *D* = *M*_w DOSY ÷ *M*_n NMR. ^g *D* = *M*_w ÷ *M*_n as determined by GPC. ^h *rac*-Lactide recrystallized from toluene was employed. ⁱ 2-Propanol was employed as co-initiator 1 : 1 Cat:ⁱPrOH. ^j Lactide/catalyst stoichiometric ratio of 50 : 1.



Zr(OⁱPr)₄·ⁱPrOH and Sn(Oct)₂ as catalysts. Surprisingly, the nature of the metal (titanium *vs.* zirconium) did not show a significant impact on the polymers generated. Amongst the unsubstituted phenolate-based ligands, complexes of **L3** (entries 4 and 11) gave the polymers with the lowest molecular weights. Surprisingly, increasing the size of the substituent on the endocyclic nitrogen from methyl to isopropyl leads to an increase in the polymer molecular weight for titanium (entries 1 *vs.* 3) but a decrease for zirconium (entries 6 *vs.* 8). The same effect was observed when large *tert*-butyl substituents were installed on the phenoxide rings, with an increase in molecular weight observed with titanium (entries 1 *vs.* 2) and a decrease with zirconium (entries 6 and 7).

While the dispersity (*D*) of all polymers was satisfactory (1.1–2.3), the observed molecular weights were approximately 70% lower than expected based on the initial monomer-to-catalyst ratio and assuming a living polymerization. Furthermore, the polymer molecular weight remains constant with conversion and deviates from the theoretical molecular weight (Fig. S57†) thus indicating chain transfer and/or transesterification. While the activity of the catalyst improved when using purified lactide, no marked improvement was observed in the molecular weight of the polymer (entry 9). The improved rate however supports the poisoning of the catalyst by impurities present in the unpurified monomer, such as lactic acid and water.⁶²

The ¹H and ¹³C NMR spectra of all polymers generated showed the incorporation of an isopropyl group as a chain end, consistent with these group 4 catalysts operating through a coordination-insertion mechanism. The competing activated monomer mechanism cannot however be ruled out based on the lower-than-expected observed relative ratio for the isopropyl to the hydroxyl end groups, which is supported by the enhanced rate in the presence of two equivalents of isopropanol (entry 10). This result further supports that nucleophilic impurities in lactide can also participate as an external initiator.

The tacticity of the polymers was determined by homonuclear-decoupled ¹H{¹H} NMR spectroscopy and all showed a heterotactic bias (*P_T* = 0.56–0.62).^{63–65} Similar heterotactic biases were observed with the related phenoxy-imine and benzoxazole-phenoxide systems, with limited to no effect of the ligand structure.^{48,66} In contrast, Ti(OⁱPr)₄ and Zr(OⁱPr)₄·ⁱPrOH showed no stereoselectivity, with a *P_T* value of 0.50, indicating that the bis(guanidine-phenolate) complexes impart some enantiomorphic-site control, albeit limited.

Given the surprisingly marginal effects of the metal and of the ligand structures on the performance of the catalysts, we became suspicious that the high temperatures used might lead to ligand dissociation. Polymerization with **L2H** (entry 13; Table 4) gave polylactide with a rate constant and molecular weights similar to those reported for the corresponding metal complexes. This supports the possible dissociation of the ligand from the metal complexes with the free guanidine actually catalyzing the ring-opening of the lactide, as previously reported for guanidines and cyclic esters.^{67,68} Complex **Zr2a** indeed decomposes in a first-order decay when heated in toluene at 120 °C, with an estimated half-life of 15 h, providing evidence

that the ligands themselves play a role in the polymerization of lactide. Unsurprisingly, **L2H** does not impart any tacticity bias.

The MALDI-TOF mass spectrometry of the PLA generated by **Ti2a**, **Zr2a**, and **L2H** had peak separations of 72 Da, evidence of transesterification which itself explains the observed low molecular weights. In addition, the spectra provide evidence of isopropyl or hydroxyl end-capped polymer chains for both **Ti2a** and **Zr2a** as catalyst, with no evidence of cyclic oligomers, further supporting a coordination-insertion mechanism. The mass spectrum of PLA generated by **L2H** does not show the incorporation of the ligand into the polymer, indicating monomer activation through a hydrogen bonding mechanism.⁶⁷

The reaction conditions used in large-scale productions were replicated more closely by increasing the lactide-to-catalyst ratio from 100 : 1 to 1000 : 1 for **Ti2a**, **Zr2a** and **L2H**. All catalysts gave polymer with the expected decrease in the pseudo first-order rate constant by approximately one order of magnitude to 1.42×10^{-5} , 2.03×10^{-5} and $0.92 \times 10^{-5} \text{ s}^{-1}$, respectively (Table S2†).

Ethylene polymerization using titanium complexes

Given the structural similarities to group 4 phenoxy-imine titanium chloride complexes,⁵⁴ **Ti1b**, **Ti1'b**, and **Ti2b** were evaluated for the polymerization of ethylene (1 atm) at room temperature with *n*-octyl-modified methylaluminoxane (MMAO-12) as cocatalyst. Titanium complex **Ti1b** and **Ti2b** gave comparable activities of $1.1 \text{ kg}_{\text{PE}} \text{ mol}_{\text{Ti}}^{-1} \text{ h}^{-1}$ and $0.8 \text{ kg}_{\text{PE}} \text{ mol}_{\text{Ti}}^{-1} \text{ h}^{-1}$ (over 1–3 hours), respectively, approximately two orders of magnitude lower than that observed with Cp₂TiCl₂ (over 3 min). The *tert*-butyl derivative **Ti1'b** gave only traces of polymer. This is in stark contrast with the 85-fold increase in activity reported when a *tert*-butyl group is installed on phenoxy-imine ligands. Fujita stated that positioning of the flanking *tert*-butyl groups above and below the reaction site (Cl–M–Cl), as in the *cis*-*N,N*-*trans*-*O,O* arrangement (isomer **A**), lowers the energy barrier for olefin insertion and mitigate side reactions.⁵⁴ The DFT calculations however predicted a *trans*-*N,N*-*cis*-*O,O* arrangement (isomer **C**; *vide supra*) for the bis(guanidine-phenolate) dichloride complexes placing the *tert*-butyl group at the back of the reaction site. Interestingly, phenoxy-imine systems that adopt this same *trans*-*N,N*-*cis*-*O,O* arrangement also showed poor activity in ethylene polymerization.^{54,58,69} The low activity of the guanidine-phenolate-based catalysts might thus be attributed to both an undesirable diastereomer and a less electrophilic metal center due to the strong electron-donating guanidine fragment.

Conclusions

The bis(guanidine-phenolate) group 4 alkoxide complexes were evaluated for the ring-opening polymerization of *rac*-lactide under solvent-free conditions and gave PLA with molecular weights and dispersity values comparable to those observed using industrial standard Sn(Oct)₂ under identical conditions. The guanidine-phenol itself seemingly also plays an important



role in the polymerization, with rates comparable to those observed with the corresponding metal complexes. PLA generated from these bis(alkoxide) complexes showed a stronger heterotactic bias compared to free ligand and the other catalysts used in control experiments. The related dichloride titanium complexes however showed poor activity in the polymerization of ethylene, even with the bulky *tert*-butyl phenolate derivative. These guanidine-phenolate ligands and the ability to further tailor its electronic and steric features offer excellent opportunities to further expand the experimental space and explore their use in other catalytic transformations. Results will be reported in due course.

Experimental section

General considerations

All manipulations and materials were performed under dry argon atmosphere, using Schlenk techniques or in a nitrogen-filled MBraun glovebox. $\text{Ti}(\text{O}^i\text{Pr})_4$, $\text{Zr}(\text{O}^i\text{Pr})_4$, $i\text{PrOH}$, $\text{TiCl}_4(\text{THF})_2$, $\text{Sn}(\text{Oct})_2$, NaHMDS , and TMSCl were purchased from Sigma-Aldrich and used without further purification. Lactide was purchased from Thermo Fisher Scientific and used as received unless otherwise stated; if needed the monomer was purified by recrystallization from toluene. 2-Amino-4,6-di-*tert*-butylphenol, 2-chloro-1-methylimidazole, **3Cl**, **4Cl**, and **L3H** were synthesized according to literature procedure.^{70,71} Deuterated solvents C_6D_6 and CDCl_3 were purchased from Sigma-Aldrich. C_6D_6 and CDCl_3 were dried over sodium and benzophenone, and over CaH_2 , respectively. Both were degassed by freeze-pump-thaw cycles, vacuum transferred to dry ampules and stored over molecular sieves prior to use.

Computational details

The calculations were performed with the computational package Gaussian 16 on Shared Hierarchical Academic Research Computing Network (SHARCNET; <https://www.sharcnet.ca/my/front/>) and made possible by Compute Canada (<https://computecanada.ca/>). SHARCNET is a consortium of colleges, universities and research institutes operating a network of high-performance computer clusters across Ontario. All geometry optimizations were performed using the B3LYP functional with the Def2SVP basis set.⁷² Grimme's empirical dispersion correction term with Becke-Johnson damping, D3(BJ) was applied.⁷³ Single point energies calculations were performed with B3LYP-D3(BJ)/Def2-TZVPP level of theory.

Crystal structure determination

Diffraction data for complexes were collected on a Bruker APEX-II CCD diffractometer with a Mo $K\alpha$ ($\lambda = 0.71073 \text{ \AA}$) radiation source. Crystals were selected under paratone oil and mounted under a stream of N_2 and kept at 173 K during data collection. Structures were solved in Olex2 (ref. 74) using direct methods and refined with SHELXL⁷⁵ refinement package using least-squares minimization.

MALDI-TOF Mass Spectrometry

MALDI-TOF MS data was obtained at the AIMS (Advanced Instrumentation for Molecular Structure) laboratory of the University of Toronto on a Bruker AutoFlex Speed MALDI-TOF mass spectrometer with a 2 kHz frequency tripled Nd:YAG laser ($\lambda = 355 \text{ nm}$). Samples were prepared in a dithranol THF matrix.

Molecular weight determination by gel permeation chromatography

Number average molar mass (M_n), weight average molar mass (M_w), and dispersity (D ; M_w/M_n) of samples (1 to 2 mg mL^{-1} in tetrahydrofuran) were determined by gel permeation chromatography (GPC) using two PLgel miniMIX-B columns ($4.6 \text{ mm} \times 250 \text{ mm}$) and two PLgel miniMIX-C columns ($4.6 \text{ mm} \times 250 \text{ mm}$) from Agilent on elution with tetrahydrofuran (0.4 mL min^{-1}) at 30°C equipped with an Agilent multi detector suite composed of an Agilent G7801A refractive index detector, an Agilent G7803A dual-angle light scattering detector and an Agilent G7802A viscometer, all of them at 30°C . The three detectors were calibrated using a narrow polystyrene standard (PS) from Agilent ($M_p = 27\,060 \text{ g mol}^{-1}$). Columns were calibrated using eight PS standards with a conventional approach (data from refractive index detector only). Data were analyzed using the Agilent GPC software version A.02.01 software (Santa Clara, CA 95051, United States).

Synthesis

1Cl. A Schlenk flask was charged with 2-chloro-1-methylimidazole (912 mg, 7.82 mmol, 1.0 equiv.) followed by the addition of 20 mL of DCM. Methyl iodide (750 mL, 11.4 mmol, 1.5 equiv.) was added dropwise. The reaction mixture was stirred for 16 h at room temperature. Volatiles were removed *in vacuo* and the solids washed with diethylether ($2 \times 10 \text{ mL}$). Volatiles were removed to give a tan solid (1.81 g, 7.02 mmol, 88%). ^1H NMR (400 MHz, CDCl_3): δ 7.97 (s, 2H, $\text{N}(\text{CH}_2\text{N})$), 4.03 (s, 6H, $\text{N}-\text{CH}_3$). ^{13}C NMR (100 MHz, CDCl_3): δ 124.4 (s, $\text{N}(\text{CH}_2\text{N})$), 37.2 (s, $\text{N}-\text{CH}_3$). Anal. calcd for $\text{C}_5\text{H}_8\text{ClIN}_2$ (%): C, 23.23; H, 3.12; N, 10.84. Found (%): C, 23.45; H, 2.96; N, 10.54.

2Cl. A round bottom flask was charged with 1,3-diisopropylimidazolium bromide (1.02 g, 4.37 mmol, 1 equiv.) following by the addition of sodium *tert*-butoxide (0.049 g, 0.437 mmol, 0.1 equiv.) and sodium hydride (0.115 g, 4.80 mmol, 1.1 equiv.) then 15 mL of THF was added and the solution stirred for 16 hours. The carbene 1,3-diisopropylimidazol-2-ylidene was extracted in THF. Subsequently, the THF solution was filtrated through Celite and slowly added to a solution containing C_2Cl_6 (1.13 g, 4.80 mmol, 1.1 equiv.) in THF at -40°C . The reaction mixture was left to reach room temperature and stirred for 24 hours. The resulting solids were filtered and washed with THF ($4 \times 5 \text{ mL}$) and dried under vacuum to yield a tan solid (819 mg, 3.67 mmol, 84%). ^1H NMR (400 MHz, CDCl_3): δ 8.38 (s, 2H, $\text{N}(\text{CH}_2\text{N})$), 4.80 (sept, $J = 6.7 \text{ Hz}$, 2H, CHMe_2), 1.64 (d, $J = 6.7 \text{ Hz}$, 12H, CHMe_2). ^{13}C (100 MHz, CDCl_3): δ 121.9 (s, $\text{N}(\text{CH}_2\text{N})$), 53.4



(s, CHMe₂), 22.2 (s, CHMe₂). Anal. calcd for C₉H₁₆Cl₂N₂ (%): C, 48.44; H, 7.23; N, 12.55. Found (%): C, 48.12; H, 7.11; N, 12.66.

L1H. A Schlenk flask was charged with 2-aminophenol (218 mg, 1.99 mmol, 1.0 equiv.) and triethylamine (0.50 mL, 4.10 mmol, 2.0 equiv.) with 20 mL of MeCN. In a separate vial, compound **1Cl** (516 mg, 1.99 mmol, 1.0 equiv.) was dissolved in 10 mL of MeCN. The solution of **1** was added and the mixture stirred under reflux for 3 h. Thereafter KOH (226 mg, 4.10 mmol, 2.1 equiv.) in 3 mL of H₂O was then added and stirred for 15 min. Volatiles were removed under vacuum. The ligand was extracted with toluene (6 × 5 mL). The combined organic layers were dried over Na₂SO₄. Removal of the volatiles *in vacuo* gave a dark yellow solid (305 mg, 1.50 mmol, 75%). ¹H NMR (300 MHz, CDCl₃): δ 6.87–6.85 (m, 1H, Ar-CH), 6.63–6.61 (m, 1H, Ar-CH), 6.26 (s, 2H, N(CH)₂N), 3.19 (s, 6H, NCH₃). ¹³C {¹H} NMR (75 MHz, CDCl₃) δ 149.4 (s, C=N), 149.1 (s, C-OH), 137.6 (s, C-N), 119.3 (s, CH-Ar), 119.1 (s, CH-Ar), 118.2 (s, CH-Ar), 114.6 (s, N(CH)₂N), 112.4 (s, CH-Ar), 33.9 (s, NCH₃). Anal. calcd for C₁₁H₁₃N₃O (%): C, 65.01; H, 6.45; N, 20.68. Found (%): C, 65.21; H, 6.06; N, 20.92.

L1H·HCl. A round-bottom flask was charged with **L1H** (150 mg, 0.738 mmol, 1 equiv.) and 10 mL of THF. Followed by the addition of a solution of HCl in dioxane (0.25 mL, 1.00 mmol, 1.4 equiv.). The mixture was stirred for 30 min, thereafter, the volatiles were removed under vacuum. The tan solid was washed with diethylether, and dried under reduced pressure (172 mg, 0.721 mmol, 97%). ¹H NMR (300 MHz, D₂O): δ 6.90–6.87 (m, 1H, Ar-CH), 6.76–6.70 (m, 1H, Ar-CH), 6.16 (s, 2H, N(CH)₂N), 3.35 (s, 6H, NCH₃). Anal. calcd for C₁₁H₁₄ClN₃O (%): C, 55.12; H, 5.89; N, 17.53. Found (%): C, 55.48; H, 5.74; N, 17.30.

L1'H. This compound was prepared by the same method as **L1H** with 2-amino-4,6-di-*tert*-butylphenol to give a green solid (205.5 mg, 0.553 mmol, 70%). ¹H NMR (300 MHz, CDCl₃): δ 6.74 (d, *J* = 3.0 Hz, 1H, CH-Ar), 6.59 (d, *J* = 3.0 Hz, 1H, CH-Ar), 6.22 (s, 2H, N(CH)₂N), 3.18 (s, 6H, NCH₃), 1.43 (s, 9H, C(CH₃)₃), 1.28 (s, 9H, C(CH₃)₃). ¹³C {¹H} NMR (75 MHz, CDCl₃) δ (s, C=N), 145.6 (s, C-OH), 139.7 (s, C-N), 136.6 (s, C-^{*t*}Bu), 132.4 (s, C-^{*t*}Bu), 114.3 (s, CH-Ar), 114.0 (s, N(CH)₂N), 113.8 (s, CH-Ar), 34.7 (s, CMe₃), 34.3 (s, NCH₃), 33.9 (s, C-Me₃), 31.9 (s, CMe₃), 29.8 (s, CMe₃). Anal. calcd for C₁₉H₂₉N₃O (%): C, 72.34; H, 9.27; N, 13.32. Found (%): C, 72.73; H, 9.15; N, 12.99.

L1'H·HCl. This compound was prepared by the same method as **L1H·HCl**, to give a tan solid (150 mg, 0.369 mmol, 97%). ¹H NMR (300 MHz, CDCl₃): δ 10.67 (s, 1H, NH) 7.15 (s, 1H, CH-Ar), 6.80 (s, 2H, N(CH)₂N), 6.58 (s, 1H, CH-Ar) 3.51 (s, 6H, NCH₃), 1.41 (s, 9H, C(CH₃)₃), 1.24 (s, 9H, C(CH₃)₃). ¹³C {¹H} NMR (75 MHz, CDCl₃) δ 147.4 (s, C=N), 143.9 (s, C-OH), 142.4 (s, C-N), 140.0 (s, C-^{*t*}Bu), 125.9 (s, C-^{*t*}Bu), 121.7 (s, CH-Ar), 118.5 (s, N(CH)₂N), 117.9 (s, CH-Ar), 35.5 (s, NCH₃), 34.3 (s, C-(Me)₃), 31.6 (s, C-(Me)₃), 29.8 (s, C-(Me)₃). Anal. calcd for C₁₉H₃₀ClN₃O (%): C, 64.85; H, 8.59; N, 11.94. Found (%): C, 64.70; H, 8.28; N, 11.75.

L2H·HCl. A Schlenk flask was charged with 2-aminophenol (300 mg, 1.99 mmol, 1.0 equiv.) and triethylamine (0.50 mL, 4.10 mmol, 2.0 equiv.) in 20 mL of MeCN. In a separated vial, compound **2Cl** (516 mg, 1.99 mmol, 1.0 equiv.) was dissolved in

10 mL of MeCN. The solution of **2Cl** was added and the mixture stirred under reflux for 6 h. Thereafter KOH (122 mg, 2.2 mmol, 1.1 equiv.) in 3 mL of H₂O was added and the solution stirred for 30 min. Volatiles were removed under vacuum. The product was extracted with THF (3 × 5 mL), then solvent was removed under vacuum to give a white solid (493.167 mmol, 84%). ¹H NMR (300 MHz, CDCl₃): δ 7.16–7.13 (m, 1H, Ar-CH), 7.03 (s, 2H, N(CH)₂N), 6.98–6.96 (m, 1H, Ar-CH), 6.77–6.72 (m, 1H, Ar-CH), 6.48–6.46 (m, 1H, Ar-CH), 4.71 (sept, *J* = 6.7 Hz, 2H, CH-Me₂), 1.40 (d, *J* = 6.7 Hz, 12H, CH-Me₂). ¹³C {¹H} NMR (75 MHz, CDCl₃) δ 149.0 (s, CH-Ar), 141.2 (s, C=N), 128.6 (s, C-OH), 125.4 (s, CH-Ar), 120.4 (s, CH-Ar), 119.9 (s, CH-Ar), 118.7 (s, C-N), 114.8 (s, N(CH)₂N), 50.1 (s, CH-^{*i*}Pr), 22.5 (s, CH-Me₂). Anal. calcd for C₁₅H₂₂ClN₃O (%): C, 60.91; H, 7.50; N, 14.21. Found (%): C, 61.29; H, 7.22; N, 14.13.

L2H. A round-bottom flask was charged with **L2H·HCl** (200 mg, 0.68 mmol, 1.0 equiv.) and 10 mL of MeCN. Follow by the addition of KOH (40 mg, 0.70 mmol, 1.05 equiv.). The mixture was stirred for 30 min. Volatiles were removed under vacuum, the product is extracted with DCM (5 mL × 3) Solvent was removed under reduce pressure to yield a brown solid (150 mg, 0.57 mmol, 85%) ¹H NMR (300 MHz, CDCl₃): δ 6.86 (m, 1H, Ar-CH), 6.67–6.59 (m, 3H, Ar-CH), 6.45 (s, 2H, N(CH)₂N), 4.44 (sept, *J* = 6.7 Hz, 2H, CH-Me₂), 1.23 (d, *J* = 6.7 Hz, 12H, CH-Me₂). ¹³C {¹H} NMR (75.46 MHz, CDCl₃) δ 149.0 (s, C=N), 147.9 (s, C-OH), 138.8 (s, C-N), 119.4 (s, CH-Ar), 118.3 (s, CH-Ar), 116.0 (s, CH-Ar), 112.3 (s, CH-Ar), 110.0 (s, N(CH)₂N), 46.3 (s, CH-^{*i*}Pr), 22.0 (s, CH₃-^{*i*}Pr). Anal. calcd for C₁₅H₂₁N₃O (%): C, 69.47; H, 8.16; N, 16.20. Found (%) C, 69.35; H, 8.10; N, 16.55.

L4H·HCl. This compound was prepared by the same method as **L2H·HCl**, to give a white solid (150 mg, 0.369 mmol, 97%). ¹H NMR (300 MHz, CDCl₃): δ 9.86 (s, 1H, NH), 9.33 (s, 1H, OH), 7.23–7.21 (m, 1H, CH-Ar) 6.99–6.97 (s, 1H, CH-Ar) 6.74–6.72 (s, 1H, CH-Ar), 3.30 (t, *J* = 6.0 Hz, 4H, NCH₂), 2.91 (s, 6H, NCH₃), 2.03 (q, *J* = 6.0 Hz, 4H, CH₂). ¹³C {¹H} NMR (75 MHz, CDCl₃) δ 155.6 (s, C=N), 150.5 (s, C-OH), 126.9 (s, CH-Ar), 126.1 (s, C-N), 123.9 (s, CH-Ar), 120.4 (s, CH-Ar), 119.0 (s, CH-Ar) 48.6 (s, N-CH₃), 40.5 (N-CH₂), 22.4 (CH₂CH₂CH₂). Anal. calcd for C₁₂H₁₈ClN₃O (%): C, 56.36; H, 7.09; N, 16.43. Found (%) C, 56.61; H, 7.22; N, 16.58.

L4H. This compound was prepared by the same method as **L2H**. ¹H NMR (400 MHz, C₆D₆): δ 7.50 (s, 1H, OH), 7.28–7.27 (m, 1H, CH-Ar) 6.99–6.97 (s, 3H, CH-Ar) 6.74–6.72 (s, 1H, CH-Ar), 2.44 (s, 6H, NCH₃), 2.41 (t, *J* = 6.0 Hz, 4H, NCH₂), 1.07 (q, *J* = 6.0 Hz, 4H, CH₂). ¹³C {¹H} NMR (100 MHz, CDCl₃) δ 155.7 (s, C=N), 150.5 (s, C-OH), 138.6 (s, C-N) 120.2 (s, CH-Ar), 119.4 (s, CH-Ar), 118.7 (s, CH-Ar), 113.1 (s, CH-Ar) 48.3 (s, N-CH₃), 39.0 (N-CH₂), 22.1 (CH₂CH₂CH₂). Anal. calcd for C₁₂H₁₇N₃O (%): C, 65.73; H, 7.81; N, 19.16. Found (%) C, 65.48; H, 7.63; N, 18.95.

Ti1a. A solution of **L1H** (105 mg, 0.517 mmol, 2.0 equiv.) in 5 mL of DCM was added to a solution of Ti(O^{*i*}Pr)₄ (73.8 mg, 0.261 mmol, 1.0 equiv.) in 5 mL of DCM. Reaction mixture was placed under reflux for 5 h. Thereafter, the solvent was removed under reduced pressure. The solid formed was washed with pentane to yield a yellow solid (125.9 mg, 0.220 mmol, 85%). ¹H NMR (400 MHz, C₆D₆): δ 6.79–6.76 (m, 1H, Ar-CH), 6.63–6.61



(m, 2H, Ar-CH), 6.03–6.00 (m, 1H, Ar-CH), 5.49 (s, 2H, N(CH)₂N), 5.28 (sept, *J* = 6.0 Hz, 1H, OCHMe₂), 3.03 (s, 6H, NCH₃), 1.37 (d, *J* = 6.0 Hz, 6H, OCHMe₂). ¹³C{¹H} NMR (100 MHz, C₆D₆) δ 160.7 (s, C=N), 153.2 (s, C-OH), 145.2 (s, C-N), 119.0 (s, CH-Ar), 116.7 (s, CH-Ar), 115.5 (s, N(CH)₂N), 113.9 (s, CH-Ar), 112.9 (s, CH-Ar), 75.6 (s, OCHMe₃), 34.3 (s, NCH₃), 26.5 (s, OCH-Me₃) δ anal. calcd for C₂₈H₃₈N₆O₄Ti (%): C, 58.95; H, 6.71; N, 14.73. Found (%) C, 59.30; H, 6.27; N, 15.22.

Ti1'a. A solution of L1'H (150 mg, 0.475 mmol, 2.0 equiv.) in 5 mL of toluene was added to a solution of Ti(OⁱPr)₄ (67.4 mg, 0.237 mmol, 1.0 equiv.) in 5 mL of toluene. Reaction mixture was placed under reflux for 5 h. Thereafter, the solvent was removed under reduced pressure. The solid formed was washed with pentane to yield a yellow solid (161 mg, 0.171 mmol, 86%). ¹H NMR (400 MHz, C₆D₆) δ 7.04 (d, *J* = 4.0 Hz, 1H, Ar-CH), 5.97 (d, *J* = 4.0 Hz, 1H, Ar-CH), 5.66–5.60 (s, 2H, N(CH)₂N), 5.46 (br, 1H, CHMe₂), 3.21 (s, 3H, NCH₃), 3.00 (s, 3H, NCH₃) 1.67 (s, 9H, C(CH₃)₃), 1.39 (s, 9H, C(CH₃)₃), 1.30 (d, *J* = 8.0 Hz, 6H, OCHMe₂). ¹³C{¹H} NMR (100 MHz, C₆D₆) δ 157.2 (s, C=N), 153.8 (s, C-OH), 145.4 (s, C-N), 137.5 (s, C-C(CH₃)₃), 133.4 (s, C-C(CH₃)₃), 116.2 (s, N(CH)₂N), 113.0 (s, CH-Ar), 108.0 (s, CH-Ar), 0.6 (s, OCHMe₃), 35.3 (s, NCH₃), 34.3 (s, C(CH₃)₃), 32.4 (s, C(CH₃)₃), 30.2 (s, C(CH₃)₃), 28.1 (s, OCH-Me₃). Anal. calcd for C₄₄H₇₀N₆O₄Ti (%): C, 66.48; H, 8.88; N, 10.57. Found (%) C, 66.61; H, 9.13; N, 10.85.

Ti2a. This compound was prepared by the same method as **Ti1'a** using L2H to yield a yellow solid (133 mg, 0.19 mmol, 89%). ¹H NMR (300 MHz, C₆D₆) δ 7.00–6.96 (m, 1H, Ar-CH), 6.82–6.79 (m, 1H, Ar-CH), 6.68–6.63 (m, 1H, Ar-CH), 6.07 (s, 1H, N(CHCH)N), 5.85–5.82 (m, 1H, Ar-CH) 5.25 (br, 2H, CH-Me₂), 4.97 (sept, 1H, *J* = 6.0 Hz, OCH-Me₂) 1.27 (d, *J* = 6.0 Hz, 6H, CH-Me₂), 1.09 (br, *J* = 6.0 Hz, 6H, OCH-Me₂), 0.95 (d, *J* = 6.0 Hz, 6H, CH-Me₂). ¹³C{¹H} NMR (76 MHz, C₆D₆) δ 158.7 (s, C=N), 150.5 (s, C-O), 145.0 (s, C-N), 117.3 (s, CH-Ar) 112.9 (s, CH-Ar), 110.9 (s, CH-Ar), 110.3 (s, N(CH)₂N) 108.5 (s, CH-Ar), 71.4 (s, OCH-Me₂), 45.9 (s, CH-Me₂), 25.0 (s, OCH-Me₂), 20.7 (s, CH-Me₂), 20.6 (s, CH₃-Me₂). Anal. calcd for C₃₆H₅₄N₆O₄Ti (%): C, 63.33; H, 7.97; N, 12.31. Found (%) C, 63.56; H, 7.66; N, 12.60.

Ti3a. This compound was prepared by the same method as **Ti1'a** using L3H to yield a yellow solid (142 mg, 0.25 mmol, 95%) ¹H NMR (400 MHz, C₆D₆) 6.86–6.80 (m, 1H, Ar-CH), 6.57–6.54 (m, 1H, Ar-CH), 6.86–6.80 (m, 1H, Ar-CH), 5.32 (sept, 1H, *J* = 6.0 Hz, OCH-Me₂), 2.65 (s, 6H, N-CH₃), 2.54 (s, 4H, N-CH₂) 1.43 (d, *J* = 6.0 Hz, 6H, CH-Me₂). ¹³C{¹H} NMR (100 MHz, C₆D₆) δ 162.1 (s, C=N), 161.3 (s, C-O), 145.2 (s, C-N), 119.7 (s, CH-Ar) 116.9 (s, CH-Ar), 116.0 (s, CH-Ar), 113.6 (s, CH-Ar), 76.3 (s, OCH-Me₂), 48.4 (s, NCH₃), 40.4 (s, N-CH₂), 26.6 (s, OCH-Me₂), 22.3 (s, CH₂). Anal. calcd for C₂₈H₄₂N₆O₄Ti (%): C, 58.53; H, 7.37; N, 14.63. Found (%) C, 58.92; H, 7.23; N, 14.46.

Ti4a. This compound was prepared by the same method as **Ti1'a** using L4H to yield a yellow solid (176 mg, 0.30 mmol, 88%). ¹H NMR (400 MHz, C₆D₆) δ 6.90–6.82 (m, 1H, Ar-CH), 6.80–6.72 (m, 2H, Ar-CH), 6.33–6.31 (m, 1H, Ar-CH), 5.37 (sept, 1H, *J* = 6.0 Hz, OCH-Me₂), 2.86 (s, 6H, N-CH₃), 2.59–2.52 (m, 2H, N-CH₂), 2.45–2.34 (m, 2H, N-CH₂), 1.48 (d, *J* = 6.0 Hz, 6H, CH-Me₂), 0.99–0.95 (m, 2H, CH₂). ¹³C{¹H} (100 MHz, C₆D₆) δ 162.1 (s, C=N), 161.3 (s, C-O), 145.2 (s, C-N), 119.7 (s, CH-Ar)

116.9 (s, CH-Ar), 116.0 (s, CH-Ar), 113.6 (s, CH-Ar), 76.3 (s, OCH-Me₂), 48.4 (s, NCH₃), 40.4 (s, N-CH₂) 26.6 (s, OCH-Me₂), 22.3 (s, CH₂). Anal. calcd for C₃₀H₄₆N₆O₄Ti (%): C, 59.80; H, 7.69; N, 13.95. Found (%) C, 60.11; H, 7.44; N, 14.19.

Zr1a. This compound was prepared by the same method as **Ti1a** using Zr(OⁱPr)₄·ⁱPrOH and L1H to yield a green solid (144 mg, 0.24 mmol, 96%). ¹H NMR (400 MHz, C₆D₆) δ 6.80–6.77 (m, 1H, Ar-CH), 6.72–6.70 (m, 1H, Ar-CH), 6.60–6.56 (m, 1H, Ar-CH), 5.98–5.96 (m, 1H, Ar-CH), 5.51 (s, 2H, N(CH)₂N), 4.62 (sept, *J* = 8.0 Hz, 1H, OCHMe₂), 2.99 (s, 6H, NCH₃), 1.37 (d, *J* = 8.0 Hz, 6H, OCHMe₂). ¹³C{¹H} NMR (100 MHz, C₆D₆) δ 159.6 (s, C=N), 153.14.88 (s, CH-Ar) 116.2 (s, CH-Ar), 115.6 (s, CH-Ar), 115.1 (s, N(CH)₂N) 114.2 (s, CH-Ar), 70.3 (s, OCH-Me₂), 34.1 (s, NCH₃), 27.0 (s, OCH-Me₂). Anal. calcd for C₂₈H₃₈N₆O₄Zr (%): C, 54.78; H, 6.24; N, 13.69. Found (%) C, 55.14; H, 6.40; N, 13.92.

Zr1'a. This compound was prepared by the same method as **Ti1'a** using Zr(OⁱPr)₄·ⁱPrOH and L1'H to yield a yellow solid (165 mg, 0.197 mmol, 92%). ¹H NMR (400 MHz, C₆D₆) δ 7.04 (d, *J* = 4.0 Hz, 1H, Ar-CH), 5.97 (d, *J* = 4.0 Hz, 1H, Ar-CH), 5.58 (s, 2H, N(CH)₂N), 4.68 (sept, *J* = 8.0 Hz 1H, CHMe₂), 3.06 (s, 6H, NCH₃), 1.70 (s, 9H, C(CH₃)₃), 1.41 (d, *J* = 8.0 Hz, 6H, OCHMe₂), 1.37 (s, 9H, C(CH₃)₃). ¹³C{¹H} NMR (100 MHz, C₆D₆) δ 156.0 (s, C=N), 153.8 (s, C-OH), 145.0 (s, C-N), 136.8 (s, C-C(CH₃)₃), 133.4 (s, C-C(CH₃)₃), 116.0 (s, N(CH)₂N), 113.0 (s, CH-Ar), 108.0 (s, CH-Ar), 69.6 (s, OCHMe₃), 35.3 (s, NCH₃), 34.3 (s, C(CH₃)₃), 32.4 (s, C(CH₃)₃), 30.2 (s, C(CH₃)₃), 28.1 (s, OCH-Me₃). Anal. calcd for C₄₄H₇₀N₆O₄Zr (%): C, 63.04; H, 8.42; N, 10.03. Found (%) C, 63.22; H, 8.13; N, 9.88.

Zr2a. This compound was prepared by the same method as **Ti2a** using Zr(OⁱPr)₄·ⁱPrOH and L2H to yield a green solid (178 mg, 0.25, 89%). ¹H NMR (300 MHz, C₆D₆) δ 7.00–6.96 (m, 1H, Ar-CH), 6.82–6.79 (m, 1H, Ar-CH), 6.68–6.63 (m, 1H, Ar-CH), 6.07 (s, 1H, N(CHCH)N), 5.85–5.82 (m, 1H, Ar-CH) 5.25 (br, 2H, CH-Me₂), 4.97 (sept, 1H, *J* = 6.0 Hz, OCH-Me₂) 1.27 (d, *J* = 6.0 Hz, 6H, CH-Me₂), 1.09 (br, *J* = 6.0 Hz, 6H, OCH-Me₂), 0.95 (d, *J* = 6.0 Hz, 6H, CH-Me₂). ¹³C{¹H} NMR (76 MHz, C₆D₆) δ 159.8 (s, C=N), 152.2 (s, C-O), 146.7 (s, C-N), 119.3 (s, CH-Ar) 115.1 (s, CH-Ar), 114.7 (s, CH-Ar), 112.2 (s, N(CH)₂N) 111.3 (s, CH-Ar), 69.3 (s, OCH-Me₂), 47.9 (s, CH-Me₂), 27.9 (s, OCH-Me₂), 23.0 (s, CH-Me₂), 22.3 (s, CH₃-ⁱPr) Anal. calcd for C₃₆H₅₄N₆O₄Zr (%): C, 59.55; H, 7.50; N, 11.57. Found (%) C, 59.26; H, 7.45; N, 11.88.

Zr3a. This compound was prepared by the same method as **Ti2a** using Zr(OⁱPr)₄·ⁱPrOH and L3H to yield a green solid (140 mg, 0.23 mmol, 93%). ¹H NMR (400 MHz, C₆D₆) δ 6.83–6.80 (m, 1H, Ar-CH), 6.70–6.67 (m, 1H, Ar-CH), 6.54–6.51 (m, 1H, Ar-CH), 4.68 (sept, 1H, *J* = 8.0 Hz, OCH-Me₂), 2.62 (s, 6H, N-CH₃), 2.49 (s, 4H, N-CH₂) 1.46 (d, *J* = 8.0 Hz, 6H, CH-Me₂). ¹³C{¹H} NMR (100 MHz, C₆D₆) δ 165.9 (s, C=N), 160.2 (s, C-O), 142.7 (s, C-N), 121.3 (s, CH-Ar) 118.4 (s, CH-Ar), 116.3 (s, CH-Ar), 115.8 (s, CH-Ar), 71.0 (s, OCH-Me₂), 47.8 (s, NCH₃), 35.6 (s, N-CH₂) 27.7 (s, OCH-Me₂). Anal. calcd for C₂₈H₄₂N₆O₄Zr (%): C, 54.43; H, 6.85; N, 13.60. Found (%) C, 54.78; H, 6.95; N, 13.76.

Zr4a. This compound was prepared by the same method as **Ti2a** using Zr(OⁱPr)₄·ⁱPrOH and L4H to yield a green solid (173 mg 0.28 mmol, 93%) ¹H NMR (400 MHz, C₆D₆) δ 6.90–6.88 (m, 1H, Ar-CH), 6.73–6.70 (m, 1H, Ar-CH), 6.30–6.28 (m, 1H,



Ar-CH), 4.72 (sept, 1H, $J = 8.0$ Hz, OCH-Me₂), 2.83 (s, 6H, N-CH₃), 2.62–2.54 (m, 2H, N-CH₂), 2.42–2.35 (m, 2H, N-CH₂), 1.51 (d, $J = 8.0$ Hz, 6H, CH-Me₂), 1.13–1.07 (m, 1H, CH₂), 1.03–0.98 (m, 1H, CH₂). ¹³C{¹H} (100 MHz, C₆D₆) δ 162.5 (s, C=N), 160.1 (s, C-O), 144.1 (s, C-N), 120.2 (s, CH-Ar) 116.3 (s, CH-Ar), 116.2 (s, CH-Ar), 115.8 (s, CH-Ar), 70.6 (s, OCH-Me₂), 48.3 (s, NCH₃), 40.1 (s, N-CH₂) 27.9 (s, OCH-Me₂), 22.2 (s, CH₂). Anal. calcd for C₃₀H₄₆N₆O₄Zr (%): C, 55.78; H, 7.18; N, 13.01. Found (%) EA C, 55.55; H, 7.03; N, 12.76.

Ti1b. A solution of LiH·HCl (150 mg, 0.62 mmol, 2.0 equiv.) in 5 mL of DCM was added to a solution of Ti(OⁱPr)₄ (88.8 mg, 0.31 mmol, 1.0 equiv.) in 5 mL of DCM. After 6 h the solvent was removed under reduced pressure. The solid was washed with pentane, solvent was removed under vacuum to yield a red solid (154 mg, 0.29 mmol, 95%). ¹H NMR (400 MHz, CDCl₃): δ 6.89 (s, 2H, N(CH₂)₂N), 6.69–6.65 (m, 1H, Ar-CH), 6.58–6.55 (m, 1H, Ar-CH), 6.45–6.44 (m, 1H, Ar-CH), 5.69–5.67 (m, 1H, Ar-CH), 3.88 (s, 3H, NCH₃), 3.72 (s, 3H, NCH₃). ¹³C{¹H} NMR (100 MHz, CDCl₃) δ 157.5 (s, C=N), 152.7 (s, C-OH), 144.4 (s, C-N), 120.3 (s, CH-Ar), 120.0 (s, CH-Ar), 118.1 (s, N(CH₂)₂N), 112.0 (s, CH-Ar), 109.2 (s, CH-Ar), 34.9 (s, NCH₃), 34.7 (s, NCH₃). Anal. calcd for C₂₂H₂₄Cl₂N₆O₂Ti (%): C, 50.50; H, 4.62; N, 16.06. Found (%) C, 50.95; H, 5.01; N, 15.63.

Ti1'b. This compound was prepared by the same method as **Ti1b** using Li¹H·HCl to yield a red solid (92.2 mg, 0.12 mmol, 92%). ¹H NMR (300 MHz, C₆D₆) δ 6.90 (d, $J = 3.0$ Hz 1H, N(CHCH)N), 6.87 (d, $J = 3.0$ Hz 1H, N(CHCH)N) 6.70 (d, $J = 3.0$ Hz, 1H, CH-Ar), 5.47 (d, $J = 3.0$ Hz, 1H, CH-Ar), 3.80 (s, 1H, NCH₃), 3.75 (s, 1H, NCH₃), 1.36 (s, 9, C(CH₃)₃), 1.20 (s, 9, C(CH₃)₃). ¹³C{¹H} NMR (76 MHz, CDCl₃) δ 153.9 (s, C=N), 153.4 (s, C-OH), 145.1 (s, C-N), 141.9 (s, CH-Ar), 131.6 (s, CH-Ar), 117.9 (s, N(CH₂)₂N), 117.6 (s, N(CH₂)₂N), 114.0 (s, CH-Ar), 104.9 (s, CH-Ar), 35.1 (s, NCH₃), 34.7 (s, NCH₃), 34.6 (s, C(CH₃)₃), 34.3 (s, C(CH₃)₃), 32.0 (s, C(CH₃)₃), 30.0 (s, C(CH₃)₃). Anal. calcd for C₃₈H₅₆Cl₂N₆O₂Ti (%): C, 61.05; H, 7.55; N, 11.24. Found (%) C, 61.33; H, 7.40; N, 11.49.

Ti2b. This compound was prepared by the same method as **Ti1b** using L2H·HCl to yield a red solid (92.4 mg, 0.107 mmol, 90%). ¹H NMR (400 MHz, CDCl₃): δ 7.00 (s, 2H, N(CH₂)₂N), 6.65–6.61 (m, 1H, CH-Ar), 6.53–6.49 (m, 1H, CH-Ar), 6.41–6.39 (m, 1H, CH-Ar), 5.63–5.61 (m, 1H, CH-Ar), 5.32 (sept, $J = 6.0$ Hz, 1H, CH-Me₂), 4.96 (sept, $J = 6.0$ Hz, 1H, CH-Me₂), 1.63 (d, $J = 6.0$ Hz, 3H, CH-Me₂), 1.51 (d, $J = 6.0$ Hz, 1H, CH-Me₂), 1.36 (d, $J = 6.0$ Hz, 1H, CH-Me₂), 1.31 (d, $J = 6.0$ Hz, 1H, CH-Me₂). ¹³C{¹H} NMR (100 MHz, CDCl₃) δ 157.8 (s, C=N), 150.2 (s, C-OH), 146.0 (s, C-N), 119.9 (s, CH-Ar), 119.6 (s, CH-Ar), 114.1 (s, N(CH₂)₂N), 114.0 (s, N(CH₂)₂N), 111.7 (s, CH-Ar), 109.0 (s, CH-Ar), 49.0 (s, CH-Me₂), 48.7 (s, CH-Me₂), 24.2 (s, CH-Me₂), 23.3 (s, CH-Me₂), 23.2 (s, CH-Me₂), 23.2 (s, CH-Me₂), 22.2 (s, CH-Me₂). Anal. calcd for C₃₀H₄₀Cl₂N₆O₂Ti (%): C, 56.70; H, 6.35; N, 13.23. Found (%) C, 56.85; H, 6.62; N, 13.44.

General procedure for the polymerization of *rac*-lactide. Otherwise specified, all polymerizations were performed using technical grade *rac*-lactide. In a typical experiment, a flask was charged with 60 μ mol of catalyst and 6.0 mmol of *rac*-lactide under inert conditions. The mixture was submerged in an oil bath at 130 °C and stirred up to 6 h. The polymerization was

cooled down to room temperature and terminated by the addition of 10 mL of wet CHCl₃. Volatiles were removed under vacuum at 50 °C for several hours. The remaining material was analyzed without further purification. Kinetic studies of solvent-free polymerization were performed under the same conditions with a [Monomer]:[Cat] ratio of 100 : 1. Aliquots were removed from the reaction mixture at different times to monitor the monomer conversion by ¹H NMR spectroscopy. Molecular weight averages were by GPC, and by end-chain analysis (M_n) and by diffusion ordered ¹H NMR spectroscopy (DOSY; M_w).

General procedure for the polymerization of ethylene. All polymerization experiments were performed under 1 atm of ethylene and at 25 °C in a 100 mL Schlenk flask charged with a stir bar. Schlenk flask was charged with 40 mL of toluene and degassed by two freeze–pump–thaw cycles. The solution was saturated with ethylene for 10 min under vigorous stirring, then treated with 4 mL (220 equiv.) of methylaluminoxane solution 7 wt% in toluene (MMAO-12). The solution was left stirring for another 15 min at which point the polymerization was initiated by the addition of a 2 mL solution of the precatalyst (40 mmol) in DCM to the flask. The reaction was quenched by the addition of 10 mL of a solution 1 : 1 of MeOH and concentrated HCl. The polymer was collected by filtration and washed with water and MeOH and dried for several hours at 60 °C under vacuum.

Data availability

The data supporting this article have been included as part of the “ESI”.† Crystallographic data for all four X-ray structures reported in the paper have been deposited to the CCDC with deposition numbers 2345354–2345357. All DFT calculations were performed using the computational package Gaussian 16 on the Shared Hierarchical Academic Research Computing Network (SHARCNET; <https://www.sharcnet.ca/my/front/>), a consortium of colleges, universities and research institutes of the province of Ontario, Canada.

Conflicts of interest

There are no conflicts to declare.

Acknowledgements

G. G. L. gratefully acknowledges financial support from the Natural Sciences and Engineering Research Council for a Discovery Grant. V. F. R thanks the Consejo Nacional de Humanidades, Ciencias y Tecnologías (CONAHCYT) of Mexico for a graduate scholarship and York University for a Carswell scholarship.

References

- 1 X. Li, Y. Lin, M. Liu, L. Meng and C. Li, *J. Appl. Polym. Sci.*, 2023, **140**, e53477.
- 2 K. Hamad, M. Kaseem, M. Ayyoob, J. Joo and F. Deri, *Prog. Polym. Sci.*, 2018, **85**, 83–127.



- 3 K. Madhavan Nampoothiri, N. R. Nair and R. P. John, *Bioresour. Technol.*, 2010, **101**, 8493–8501.
- 4 S. Mecking, *Angew. Chem., Int. Ed.*, 2004, **43**, 1078–1085.
- 5 T. A. Swetha, A. Bora, K. Mohanrasu, P. Balaji, R. Raja, K. Ponnuchamy, G. Muthusamy and A. Arun, *Int. J. Biol. Macromol.*, 2023, **234**, 123715.
- 6 V. H. Sangeetha, H. Deka, T. O. Varghese and S. K. Nayak, *Polym. Compos.*, 2018, **39**, 81–101.
- 7 A.-C. Albertsson and M. Hakkarainen, *Science*, 2017, **358**, 872–873.
- 8 C.-S. Ha and J. A. Gardella, *Chem. Rev.*, 2005, **105**, 4205–4232.
- 9 A.-C. Albertsson and I. K. Varma, *Biomacromolecules*, 2003, **4**, 1466–1486.
- 10 B. N. Mankaev and S. S. Karlov, *Materials*, 2023, **16**, 6682.
- 11 U. Yolsal, P. J. Shaw, P. A. Lowy, R. Chamenahalli and J. A. Garden, *ACS Catal.*, 2024, **14**, 1050–1074.
- 12 R. P. Singh, S. Sinhababu and N. P. Mankad, *ACS Catal.*, 2023, **13**, 12519–12542.
- 13 Y. Hu, W. Daoud, K. Cheuk and C. Lin, *Materials*, 2016, **9**, 133.
- 14 A. Kowalski, J. Libiszowski, A. Duda and S. Penczek, *Macromolecules*, 2000, **33**, 1964–1971.
- 15 H. R. Kricheldorf, I. Kreiser-Saunders and A. Stricker, *Macromolecules*, 2000, **33**, 702–709.
- 16 A. Kowalski, A. Duda and S. Penczek, *Macromolecules*, 2000, **33**, 7359–7370.
- 17 X. Zhang, D. A. MacDonald, M. F. A. Goosen and K. B. McAuley, *J. Polym. Sci., Part A: Polym. Chem.*, 1994, **32**, 2965–2970.
- 18 J. Lunt, *Polym. Degrad. Stab.*, 1998, **59**, 145–152.
- 19 K. Devaine-Pressing, F. J. Oldenburg, J. P. Menzel, M. Springer, L. N. Dawe and C. M. Kozak, *Dalton Trans.*, 2020, **49**, 1531–1544.
- 20 M. Fernández-Millán, P. Ortega, T. Cuenca, J. Cano and M. E. G. Mosquera, *Organometallics*, 2020, **39**, 2278–2286.
- 21 J. Hu, C. Kan, H. Wang and H. Ma, *Macromolecules*, 2018, **51**, 5304–5312.
- 22 Y. Wang, X. Wang, W. Zhang and W.-H. Sun, *Organometallics*, 2023, **42**, 1680–1692.
- 23 R. Duan, C. Hu, X. Li, X. Pang, Z. Sun, X. Chen and X. Wang, *Macromolecules*, 2017, **50**, 9188–9195.
- 24 S. Impemba, G. Manca, I. Tozio and S. Milione, *Polymers*, 2023, **15**, 4366.
- 25 W. Gruska, L. C. Walker, M. P. Shaver and J. A. Garden, *Macromolecules*, 2020, **53**, 4294–4302.
- 26 R. D. Rittinghaus, P. M. Schäfer, P. Albrecht, C. Conrads, A. Hoffmann, A. N. Ksiazkiewicz, O. Bienemann, A. Pich and S. Herres-Pawlis, *ChemSusChem*, 2019, **12**, 2161–2165.
- 27 M. Shaik, J. Peterson and G. Du, *Macromolecules*, 2019, **52**, 157–166.
- 28 S. Kernbichl, M. Reiter, D. H. Bucalon, P. J. Altmann, A. Kronast and B. Rieger, *Inorg. Chem.*, 2018, **57**, 9931–9940.
- 29 T. Ebrahimi, D. C. Aluthge, S. G. Hatzikiriakos and P. Mehrkhodavandi, *Macromolecules*, 2016, **49**, 8812–8824.
- 30 A. Thevenon, C. Romain, M. S. Bennington, A. J. P. White, H. J. Davidson, S. Brooker and C. K. Williams, *Angew. Chem., Int. Ed.*, 2016, **55**, 8680–8685.
- 31 S. Impemba and S. Milione, *Inorg. Chim. Acta*, 2024, **568**, 122067.
- 32 A. Buchard, C. J. Chuck, M. G. Davidson, G. Gobius Du Sart, M. D. Jones, S. N. McCormick and A. D. Russell, *ACS Catal.*, 2023, **13**, 2681–2695.
- 33 R. Hador, M. Shuster, S. Lipstman and M. Kol, *ACS Catal.*, 2022, **12**, 4872–4879.
- 34 B. J. O'Keefe, M. A. Hillmyer and W. B. Tolman, *J. Chem. Soc., Dalton Trans.*, 2001, 2215–2224.
- 35 P. Dubois, C. Jacobs, R. Jérôme and P. Teyssié, *Macromolecules*, 1991, **24**, 2266–2270.
- 36 P. Dubois, R. Jérôme and P. Teyssié, *Makromol. Chem., Macromol. Symp.*, 1991, **42–43**, 103–116.
- 37 H. R. Kricheldorf, M. Berl and N. Scharnagl, *Macromolecules*, 1988, **21**, 286–293.
- 38 P. Dobrzynski, J. Kasperczyk, H. Janeczek and M. Bero, *Macromolecules*, 2001, **34**, 5090–5098.
- 39 I. El-Zoghbi, T. J. J. Whitehorne and F. Schaper, *Dalton Trans.*, 2013, **42**, 9376–9387.
- 40 L.-J. Wu, W. Lee, P. Kumar Ganta, Y.-L. Chang, Y.-C. Chang and H.-Y. Chen, *Coord. Chem. Rev.*, 2023, **475**, 214847.
- 41 R. Dai and P. L. Diaconescu, *Dalton Trans.*, 2019, **48**, 2996–3002.
- 42 C. B. Durr and C. K. Williams, *Inorg. Chem.*, 2018, **57**, 14240–14248.
- 43 A. Sauer, A. Kapelski, C. Fliedel, S. Dagorne, M. Kol and J. Okuda, *Dalton Trans.*, 2013, **42**, 9007–9023.
- 44 C. Nakornkhet, T. Nanok, W. Wattanathana, P. Chuawong and P. Hormnirun, *Inorg. Chem.*, 2022, **61**, 7945–7963.
- 45 K. Upitak, W. Wattanathana, T. Nanok, P. Chuawong and P. Hormnirun, *Dalton Trans.*, 2021, **50**, 10964–10981.
- 46 D. J. Gilmour, R. L. Webster, M. R. Perry and L. L. Schafer, *Dalton Trans.*, 2015, **44**, 12411–12419.
- 47 A. J. Chmura, M. G. Davidson, M. D. Jones, M. D. Lunn and M. F. Mahon, *Dalton Trans.*, 2006, 887–889.
- 48 A. J. Chmura, D. M. Cousins, M. G. Davidson, M. D. Jones, M. D. Lunn and M. F. Mahon, *Dalton Trans.*, 2008, 1437–1443.
- 49 T. G. Larocque, S. Dastgir and G. G. Lavoie, *Organometallics*, 2013, **32**, 4314–4320.
- 50 B. S. Khan, V. Flores-Romero, J. LeBlanc and G. G. Lavoie, *Organometallics*, 2022, **41**, 2668–2677.
- 51 P. M. Schäfer and S. Herres-Pawlis, *ChemPlusChem*, 2020, **85**, 1044–1052.
- 52 M. Li, X. Shu, Z. Cai and M. S. Eisen, *Organometallics*, 2018, **37**, 1172–1180.
- 53 M. Li, Z. Cai and M. S. Eisen, *Organometallics*, 2018, **37**, 4753–4762.
- 54 H. Makio, H. Terao, A. Iwashita and T. Fujita, *Chem. Rev.*, 2011, **111**, 2363–2449.
- 55 E. F. Connor, T. R. Younkin, J. I. Henderson, A. W. Waltman and R. H. Grubbs, *Chem. Commun.*, 2003, 2272–2273.
- 56 T. R. Younkin, E. F. Connor, J. I. Henderson, S. K. Friedrich, R. H. Grubbs and D. A. Bansleben, *Science*, 2000, **287**, 460–462.
- 57 A. L. Johnson, M. G. Davidson, M. D. Lunn and M. F. Mahon, *Eur. J. Inorg. Chem.*, 2006, 3088–3098.



- 58 Z. Flisak, *J. Mol. Catal. A: Chem.*, 2010, **316**, 83–89.
- 59 J. L. Espartero, I. Rashkov, S. M. Li, N. Manolova and M. Vert, *Macromolecules*, 1996, **29**, 3535–3539.
- 60 H. R. Kricheldorf, I. Kreiser-Saunders and C. Boettcher, *Polymer*, 1994, **36**, 1253–1259.
- 61 P. Lewinski, S. Sosnowski, S. Kazmierski and S. Penczek, *Polym. Chem.*, 2015, **6**, 4353–4357.
- 62 O. Dechy-Cabaret, B. Martin-Vaca and D. Bourissou, *Chem. Rev.*, 2004, **104**, 6147–6176.
- 63 M. H. Chisholm, S. S. Iyer, D. G. McCollum, M. Pagel and U. Werner-Zwanziger, *Macromolecules*, 1999, **32**, 963–973.
- 64 M. T. Zell, B. E. Padden, A. J. Paterick, K. A. M. Thakur, R. T. Kean, M. A. Hillmyer and E. J. Munson, *Macromolecules*, 2002, **35**, 7700–7707.
- 65 T. M. Ovitt and G. W. Coates, *J. Am. Chem. Soc.*, 2002, **124**, 1316–1326.
- 66 S. Pappuru, V. Ramkumar and D. Chakraborty, *Polym. Adv. Technol.*, 2021, **32**, 3392–3401.
- 67 A. Chuma, H. W. Horn, W. C. Swope, R. C. Pratt, L. Zhang, B. G. G. Lohmeijer, C. G. Wade, R. M. Waymouth, J. L. Hedrick and J. E. Rice, *J. Am. Chem. Soc.*, 2008, **130**, 6749–6754.
- 68 R. C. Pratt, B. G. G. Lohmeijer, D. A. Long, R. M. Waymouth and J. L. Hedrick, *J. Am. Chem. Soc.*, 2006, **128**, 4556–4557.
- 69 J. Strauch, T. H. Warren, G. Erker, R. Frohlich and P. Saarenketo, *Inorg. Chim. Acta*, 2000, **300–302**, 810–821.
- 70 F. Bellina, M. Lessi, G. Marianetti and A. Panattoni, *Tetrahedron Lett.*, 2015, **56**, 3855–3857.
- 71 M. Baltrun, F. A. Watt, R. Schoch, C. Wölper, A. G. Neuba and S. Hohloch, *Dalton Trans.*, 2019, **48**, 14611–14625.
- 72 M. J. Frisch, G. W. Trucks, H. B. Schlegel, G. E. Scuseria, M. A. Robb, J. R. Cheeseman, G. Scalmani, V. Barone, G. A. Petersson, H. Nakatsuji, X. Li, M. Caricato, A. Marenich, J. Bloino, B. G. Janesko, R. Gomperts, B. Mennucci, H. P. Hratchian, J. V. Ortiz, A. F. Izmaylov, J. L. Sonnenberg, D. Williams-Young, F. Ding, F. Lipparini, F. Egidi, J. Goings, B. Peng, A. Petrone, T. Henderson, D. Ranasinghe, V. G. Zakrzewski, J. Gao, N. Rega, G. Zheng, W. Liang, M. Hada, M. Ehara, K. Toyota, R. Fukuda, J. Hasegawa, M. Ishida, T. Nakajima, Y. Honda, O. Kitao, H. Nakai, T. Vreven, K. Throssell, J. A. Montgomery, J. E. Peralta, F. Ogliaro, M. Bearpark, J. J. Heyd, E. Brothers, K. N. Kudin, V. N. Staroverov, T. Keith, R. Kobayashi, J. Normand, K. Raghavachari, A. Rendell, J. C. Burant, S. S. Iyengar, J. Tomasi, M. Cossi, J. M. Millam, M. Klene, C. Adamo, R. Cammi, J. W. Ochterski, R. L. Martin, K. Morokuma, O. Farkas, J. B. Foresman and D. J. Fox, *Gaussian 16, Revision C.01*, Gaussian, Inc., Wallingford, CT, 2016.
- 73 S. Grimme, J. Antony, S. Ehrlich and H. Krieg, *J. Chem. Phys.*, 2010, **132**, 154104–154122.
- 74 O. V. Dolomanov, L. J. Bourhis, R. J. Gildea, J. A. K. Howard and H. Puschmann, *J. Appl. Crystallogr.*, 2009, **42**, 339–341.
- 75 G. M. Sheldrick, *Acta Crystallogr.*, 2015, **C71**, 3–8.

